

2006

# Three-Crankshaft-Driven Scroll Compressor

Pierre Ginies

*Danfoss Commercial Compressor Division*

Christophe Ancel

*Danfoss Commercial Compressor Division*

Remi Bou Dargham

*Danfoss Commercial Compressor Division*

Follow this and additional works at: <https://docs.lib.purdue.edu/icec>

---

Ginies, Pierre; Ancel, Christophe; and Dargham, Remi Bou, "Three-Crankshaft-Driven Scroll Compressor" (2006). *International Compressor Engineering Conference*. Paper 1773.

<https://docs.lib.purdue.edu/icec/1773>

This document has been made available through Purdue e-Pubs, a service of the Purdue University Libraries. Please contact [epubs@purdue.edu](mailto:epubs@purdue.edu) for additional information.

Complete proceedings may be acquired in print and on CD-ROM directly from the Ray W. Herrick Laboratories at <https://engineering.purdue.edu/Herrick/Events/orderlit.html>

# THREE-CRANKSHAFT-DRIVEN SCROLL COMPRESSOR

Pierre GINIES, Christophe ANCEL, Rémi BOU DARGHAM

Danfoss Commercial Compressors, New Product Engineering,  
Trévoux, FRANCE

(Phone 00 33 (0)4 74 00 95 57 , Fax 00 33 (0)4 74 00 95 97 , E-mail p.ginies@danfoss.com)

## ABSTRACT

The following paper details the results of a study about the motion of an orbiting scroll in a scroll compressor. The orbiting scroll orbital motion is generated and guided by three shafts. One shaft acting as the motion generator and the other two being used to keep and maintain the orbiting motion.

The first part of the paper presents the mathematical model used for the kinematic motion and the formulae to solve it. The impact of the bearings clearances and the bearings locations tolerances are presented in the second part.

The results are plotted on charts using the differences between the theoretical orbiting motion and the actual orbiting scroll orbital trajectory completing a full rotation.

These charts make it possible to identify and detail the contacts locations history between the orbiting scroll bearings and the crankshafts, hence the motion obtained in this particular case.

## 1. INTRODUCTION

Many systems can be used to drive the mobile parts of a scroll compressor. The motion of the mobile scroll in relation to the fixed scroll must be an orbital trajectory.

The classical assembly works with a simple orbiting motion, and the design consists of a mobile scroll driven by a central crankshaft end pin, whose eccentricity is equal to the orbit radius. A coupling device prevents the rotation of the mobile scroll to secure an orbiting trajectory. For example, an Oldham coupling can be used to prevent the mobile scroll from rotating. The crankshaft is usually aligned with the central axis of the fixed scroll. The rotor is often shrink-fitted on the crankshaft, thus the motor axis is also aligned with the fixed scroll axis.

The goal of this study is to investigate the classical orbiting design with a driving and coupling system which consists of 3 crankshafts. One of the crankshaft is a driving master shaft, while the other two are slave coupling shafts and are anti-rotation devices. These crankshafts may be located at the periphery of the mobile scroll plate, allowing a side mounting of the motor.

## 2. FORCES ON THE MOBILE SCROLL

### 2.1 Location of gas and inertia forces

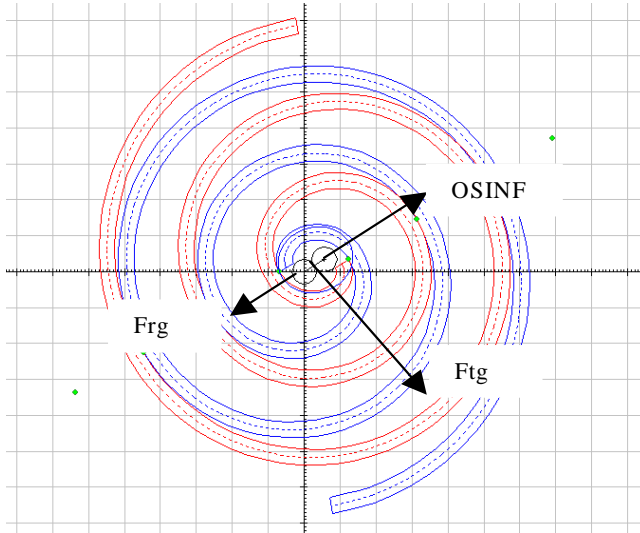


Figure 1 : the scroll geometry

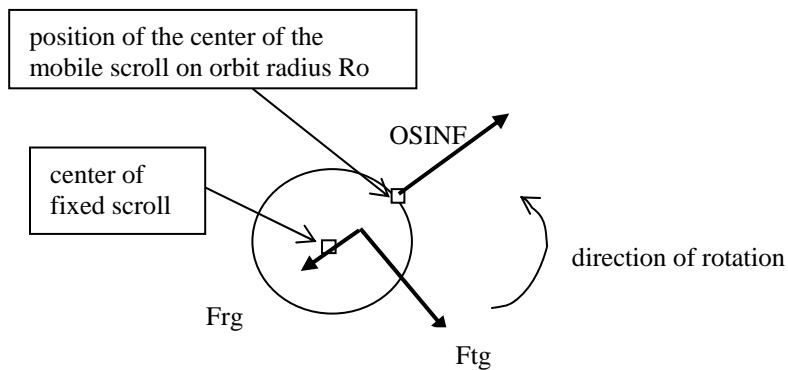


Figure 2 : the gas and inertia forces on the mobile scroll

The direction defined by the eccentric shafts is the same as the direction symbolized by the pockets sealing points line. This direction always corresponds to the imaginary line passing through both the center of the fixed scroll and the center of the mobile scroll.

The following forces are considered :

- \* the tangential compression gas force  $F_{tg}$  applies midway of the orbit radius,
- \* the radial compression gas force  $F_{rg}$  applies in a direction opposed to the mobile scroll center direction,
- \* the inertia force of the mobile scroll  $OSINF$  applies in the mobile scroll center direction.

### 2.2 Location of other forces

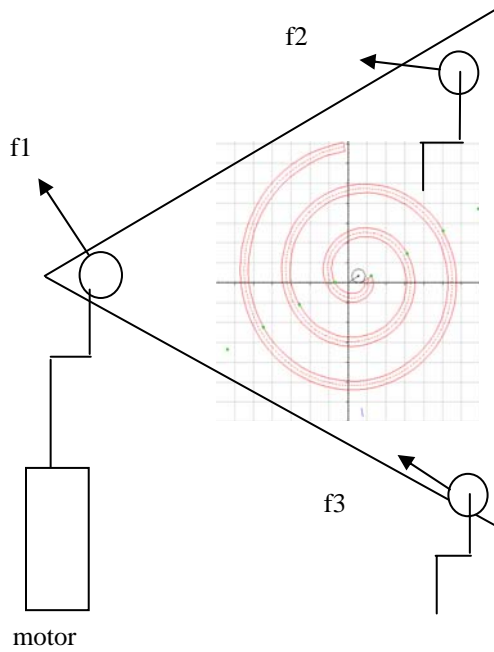


Figure 3 : the mobile scroll assembly

- $f_1$  is a combination of the drive force and of a reaction force.  $f_2$  and  $f_3$  are reaction forces. See Figure 3.

### 2.3 Modelization of the bushings clearances

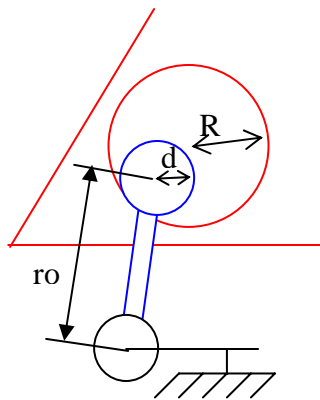


Figure 4 : the shaft and bore of the mobile scroll

- To modelize the tolerance between each eccentric pin and mobile scroll bushing, each crankshaft pin is modelized by a cylinder of radius  $d$ , while each bore of the mobile scroll plate is modelized by a hole of radius  $R$ . See Figure 4.

## 3. SOLVING

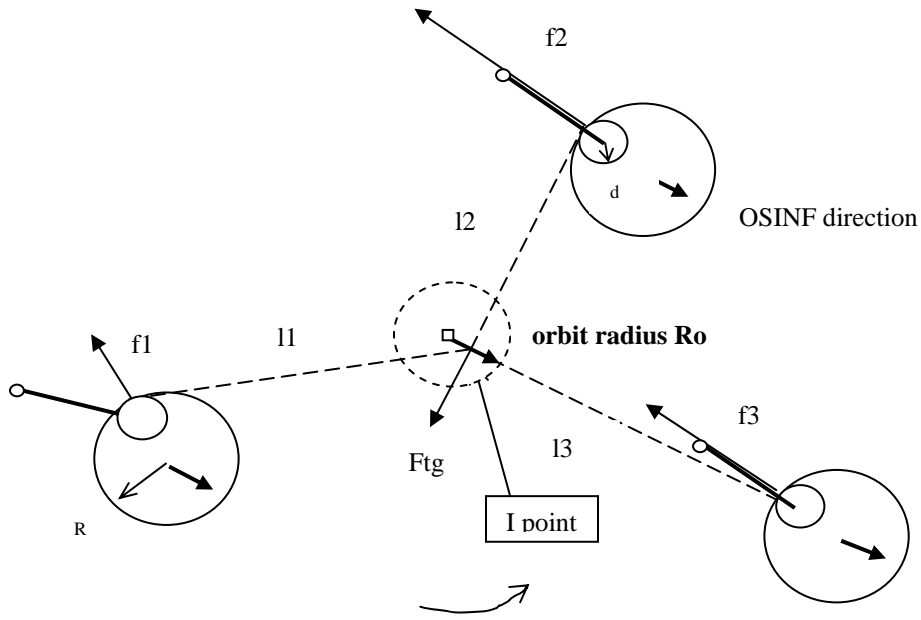


Figure 5 : the forces on the mobile scroll

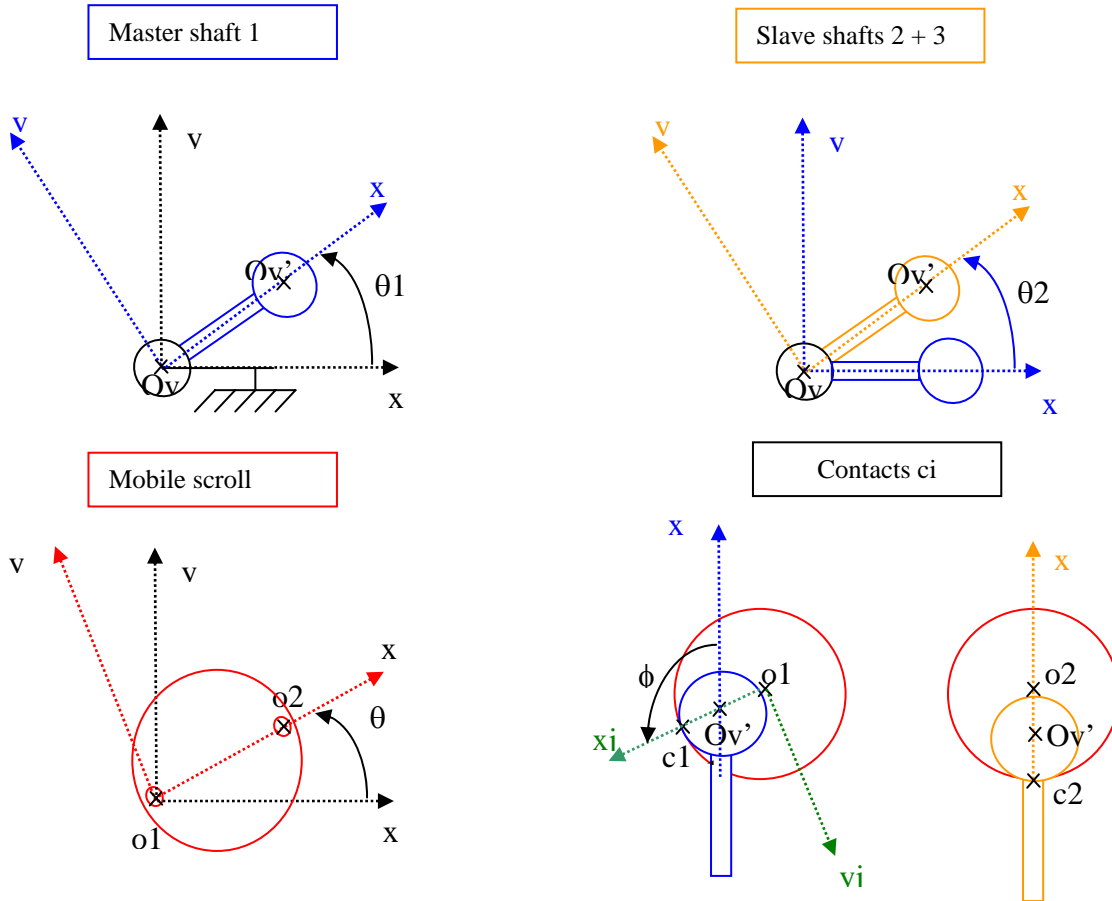


Figure 6 : the modelization parameters

Every contact point  $c_i$  is such that the applied force in  $c_i$  is perpendicular to the tangent contact line (see Figure 6). The force vectors  $f_2$  or  $f_3$  are aligned with the slave shafts, since no power is transmitted (see Figure 5). The momentum equation can be written advantageously at I point in relation to distances  $l_1$ ,  $l_2$  and  $l_3$ .

The kinematic unknowns can be represented by the angles of the shafts  $\theta_1$ ,  $\theta_2$ ,  $\theta_3$ .  $\theta$  is the slanting inclination of the mobile scroll due to the assembly clearances. If there is no clearance between the pins of shafts and the bores of the mobile scroll i.e.  $R = d$ , then  $\theta = 0$ .

To simplify the solution procedure,  $\theta_2$  and  $\theta_3$  are redefined as differential variables :

$$\theta_2 = \text{actual } \theta_2 - \theta_1$$

$$\theta_3 = \text{actual } \theta_3 - \theta_1$$

If  $\theta_2$ ,  $\theta_3$  and  $\theta$  are small, it is possible to change  $\cos \theta_i$  into 1 and  $\sin \theta_i$  into  $\theta_i$  through a limited development. This allows the linearization of the equations.

$\phi$  is the angle of the contact point following Figure 6 (see Contacts  $c_i$ ).

All coordinates are given in the absolute system. The  $(x_i, y_i)$  coordinates are those of a point of subscript  $i$  in the absolute system, while the  $(v_i, w_i)$  coordinates are in the mobile scroll coordinate system.  $(x_c, y_c)$  is the coordinate of the center of the mobile scroll.

Contact equations (hereafter for shaft 2) :

Let  $c = \cos(\theta_1)$  and  $s = \sin(\theta_1)$

$$(R-d) + [(x_2 - x_1) + (v_1 - v_2)] * c + [(y_2 - y_1) + (w_1 - w_2)] * s + [-(w_1 - w_2) * c + (v_1 - v_2) * s] * \theta + (R-d) * \cos(\phi) = 0 \quad (1)$$

$$(r_o + R - d) * \theta_2 - [(x_2 - x_1) + (v_1 - v_2)] * s + [(y_2 - y_1) + (w_1 - w_2)] * c + [(w_1 - w_2) * s + (v_1 - v_2) * c] * \theta + (R-d) * \sin(\phi) = 0 \quad (2)$$

Actual orbital radius

$$r_{actual} = \sqrt{\frac{[(v_2 - x_c) * \cos(\theta) - (w_2 - y_c) * \sin(\theta) - (r_o + R - d) * \cos(\theta_2 + \theta_1) + v_c - x_2]^2}{+ [(v_2 - x_c) * \sin(\theta) + (w_2 - y_c) * \cos(\theta) - (r_o + R - d) * \sin(\theta_2 + \theta_1) + w_c - y_2]^2}} \quad (3)$$

Force on shaft 2

$$f_2 = \frac{f_{tg} + m * r_o * \omega^2 * \tan(\phi)}{\theta_2 - \tan(\phi)} \quad (4)$$

The equations were solved using a numerical program based on the MATHCAD formulae interpreter. Imaginary numbers and non physical solutions were eliminated.

## 4. RESULTS

### 4.1 Mechanical behavior with perfect shaft axis location

Using typical clearance values for the bushings, the geometry is solved and it appears to be not compatible with permanent contacts between all mobile scroll bores and all shafts pins. Uncompatible situations are detected by the absence of positive contacts in points  $c_i$ . For classical assembly values e.g. for  $r_o = 7.08$  mm,  $R = 60.1$ mm and

$d = 60$  mm, that is to say a 0.1 mm clearance gap between the shaft pin and the mobile scroll bore, this often occurs if the  $F_{tg}/OSINF$  ratio is greater than 0.5.

The Figure 7 below shows the contact zones for each crankshaft over a full rotation of the motor shaft 1 with  $R_o = 7.08$  mm,  $R = 60.1$  mm and  $d = 60$  mm. The mobile scroll is in contact with cranshaft 1 all the time. But there are two particular angles for which the mobile scroll is completely supported by the master shaft 1 (every  $180^\circ$ ), while there are two particular angles for which the scroll is in contact with both slave crankshafts 2 and 3 (every  $180^\circ$ ).

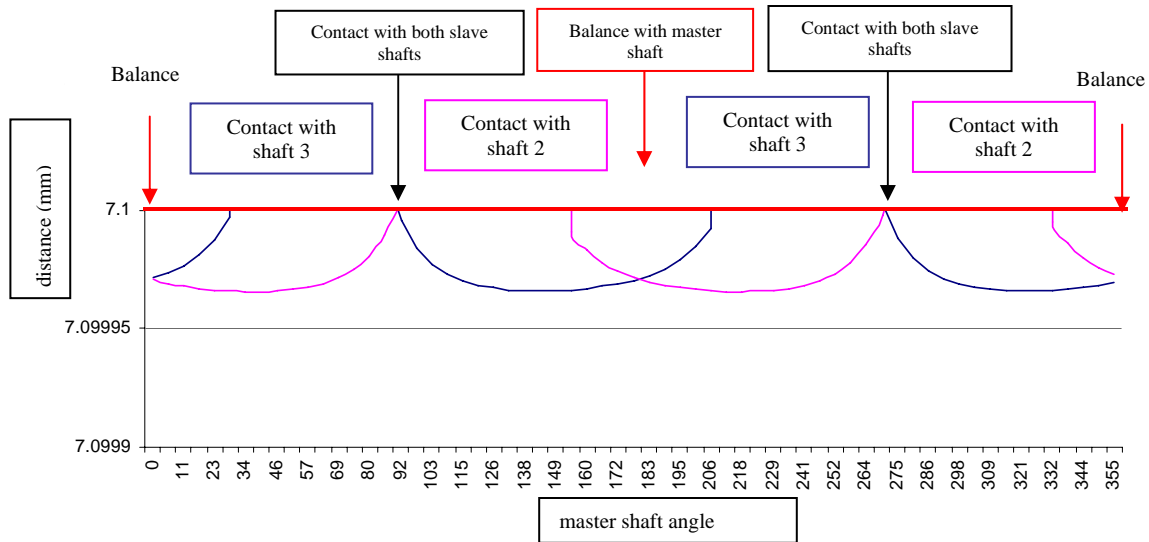


Figure 7: contact diagram for classical clearances and perfect axis location

- In Figure 8 below, a curve in implicit coordinates  $f(x,y)$  can be drawn from the above study in order to show the deviation from the ideal orbit radius over one full rotation of master shaft 1.

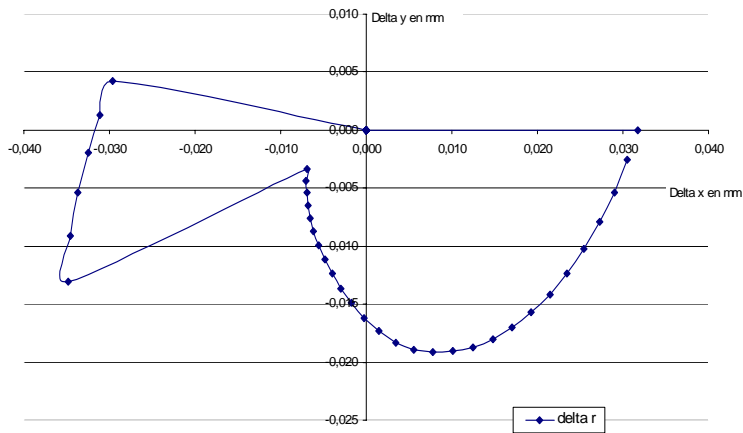


Figure 8 : distance between actual and ideal orbit radiuses

- In the same way, in Figure 9 below, the curve of orbit radius versus the angle of the master shaft 1 can be drawn and this shows clearly a 0.09 mm gap that occurs when the load switches from one shaft to another shaft. The value of the gap is close to the value of the bushing clearance (0.1 mm). The ideal orbital radius is 7.08 mm.

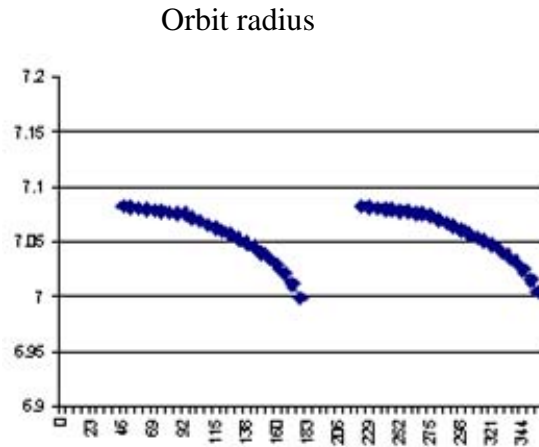


Figure 9 : curve of the orbit radius

#### 4.2 Mechanical behavior with a shaft axis offset

The triangle built with the centers of rotation of the shafts is not exactly similar to the triangle built with the centers of the bores of the mobile scroll because of the location tolerances.

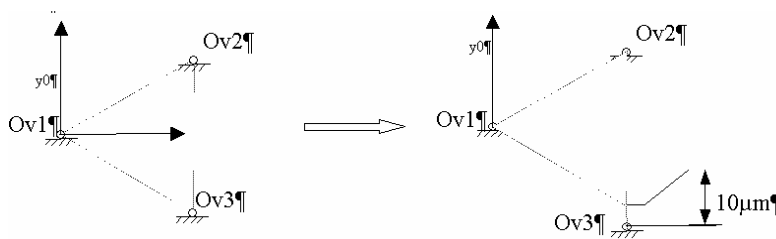


Figure 10 : offset for axis of shaft 3

Introducing an offset  $e = 10 \mu\text{m}$  for shaft 3 following Figure 10 leads to new contact equations :

The equations (5) and (6) stand for the contact between the mobile scroll and the pin of the shaft 2 :

$$\cos(\theta_1) \cdot (R - d) \cdot (\cos(\phi) + 1) - \sin(\theta_1) \cdot [(R - d) \cdot \sin(\phi) + (e + R - d) \cdot \theta_2] + (x_2 - x_1) + (v_1 - v_2) - \theta \cdot (w_1 - w_2) = 0 \quad (5)$$

$$\sin(\theta_1) \cdot (R - d) \cdot (\cos(\phi) + 1) + \cos(\theta_1) \cdot [(R - d) \cdot \sin(\phi) + (e + R - d) \cdot \theta_2] + (y_2 - y_1) + (w_1 - w_2) + \theta \cdot (v_1 - v_2) = 0 \quad (6)$$



The equations (7) and (8) stand for the contact between the mobile scroll and the pin of the shaft 3 :

$$\cos(\theta_1) \cdot (R - d) \cdot (\cos(\phi) + 1) - \sin(\theta_1) \cdot [(R - d) \cdot \sin(\phi) + (e + R - d) \cdot \theta_3] + (x_3 - x_1) + (v_1 - v_3) - \theta \cdot (w_1 - w_3) = 0 \quad (7)$$

$$\sin(\theta_1) \cdot (R - d) \cdot (\cos(\phi) + 1) + \cos(\theta_1) \cdot [(R - d) \cdot \sin(\phi) + (e + R - d) \cdot \theta_3] + (y_3 - y_1) + (w_1 - w_3) + \theta \cdot (v_1 - v_3) = 0 \quad (8)$$

Using typical clearance values for the axis location, the geometry is again not compatible with permanent contact between the shaft pins and the mobile scroll bores. The Figure 11 below shows discontinuous contacts which lead to a deviation from the ideal orbital radius.

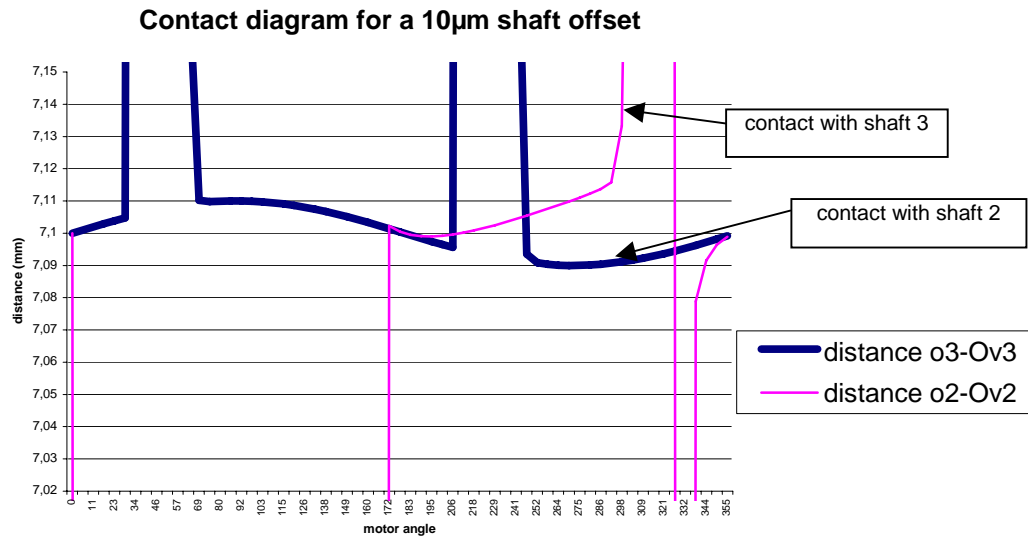


Figure 11: contact diagram for classical clearances and axis offset

## 5. CONCLUSION

The drive of a mobile scroll using three crankshafts is technically possible but it is very sensitive to the clearance between the shafts pins and the mobile scroll bushings. It is also very sensitive to any axis offset. With classical design values, this leads to a non negligible deviation from the ideal orbital radius. This deviation can result in a poor sealing between the fixed and mobile involutes, thus leaks can appear and decrease the efficiency of the compressor. This is why it is necessary to improve the three-crankshaft mechanism in order to avoid these possible problems.